Supporting Information

Energy Differences as Descriptors for the Correlation between J_{SC} and V_{OC} in Nonfullerene Organic Photovoltaics

Yue Ren[a], Ming-Yang Li[a], Ming-Yue Sui[a], Guang-Yan Sun [a,b,*], and Zhong-Min Su [a,c,*]

[a.] *Department of Chemistry, Faculty of Science, Yanbian University, Yanji 133002, P. R. China. Email:* gysun@ybu.edu.cn (Guang-Yan Sun)

[b.] *School of Applied Chemistry and Materials, Zhuhai College of Science and Technology, Zhuhai 519041, P. R. China.*

[c.] *Laboratory of Theoretical and Computational Chemistry, Institute of Theoretical Chemistry, College of Chemistry, Jilin University, Changchun 130023, P. R. China. Email:* zmsu@nenu.edu.cn (Zhong-Min Su)

*Co-first department: the **two departments** of Zhuhai College of Science and Technology and Yanbian University contributed equally to this work.*

Table of Contents

* Corresponding author.

Email: gysun@ybu.edu.cn (Guang-Yan Sun)

* Corresponding author.

Email: zmsu@nenu.edu.cn (Zhong-Min Su)

Co-first department: the two departments of Zhuhai College of Science and Technology and Yanbian University contributed equally to this work.

I. Calculation Results

$$
\begin{aligned}
\Delta E_{\mathrm{g}} &= (E_g)_2 - (E_g)_1 \\
&= (E_{\mathrm{LUMO}}^{\mathrm{A_2}} - E_{\mathrm{HOMO}}^{\mathrm{A_2}}) - (E_{\mathrm{LUMO}}^{\mathrm{A_1}} - E_{\mathrm{HOMO}}^{\mathrm{A_1}}) \\
&= (E_{\mathrm{LUMO}}^{\mathrm{A_2}} - E_{\mathrm{LUMO}}^{\mathrm{A_1}}) - (E_{\mathrm{HOMO}}^{\mathrm{A_2}} - E_{\mathrm{HOMO}}^{\mathrm{A_1}}) \\
&= \Delta E_{\mathrm{LUMO}} - \Delta E_{\mathrm{HOMO}} \\
\Delta(\Delta E_1) &= (\Delta E_1)_2 - (\Delta E_1)_1 \\
&= (E_{\mathrm{LUMO}}^{\mathrm{D}} - E_{\mathrm{LUMO}}^{\mathrm{A_2}}) - (E_{\mathrm{LUMO}}^{\mathrm{D}} - E_{\mathrm{LUMO}}^{\mathrm{A_1}}) \\
&= E_{\mathrm{LUMO}}^{\mathrm{A_1}} - E_{\mathrm{LUMO}}^{\mathrm{A_2}} \\
&= -\Delta E_{\mathrm{LUMO}}
\end{aligned}
\qquad \text{S1}
$$

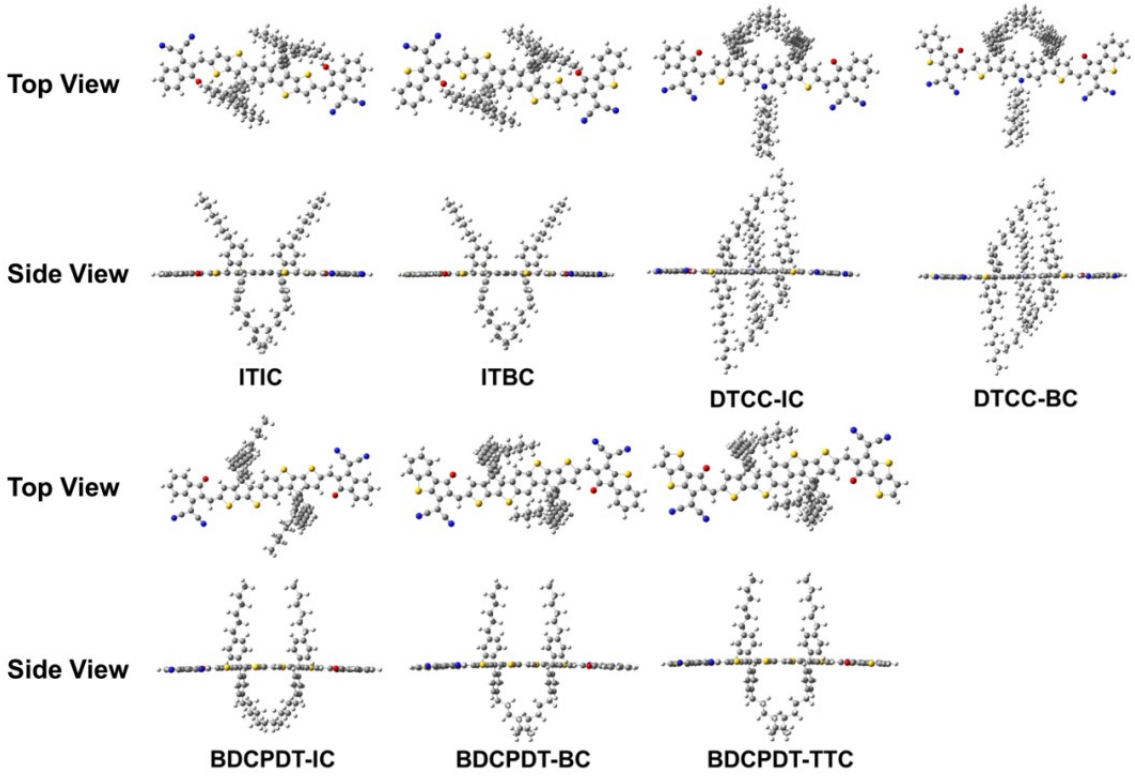

Figure S1. The most stable monomeric conformations of ITIC-series acceptors are optimized adopted density functional theory.

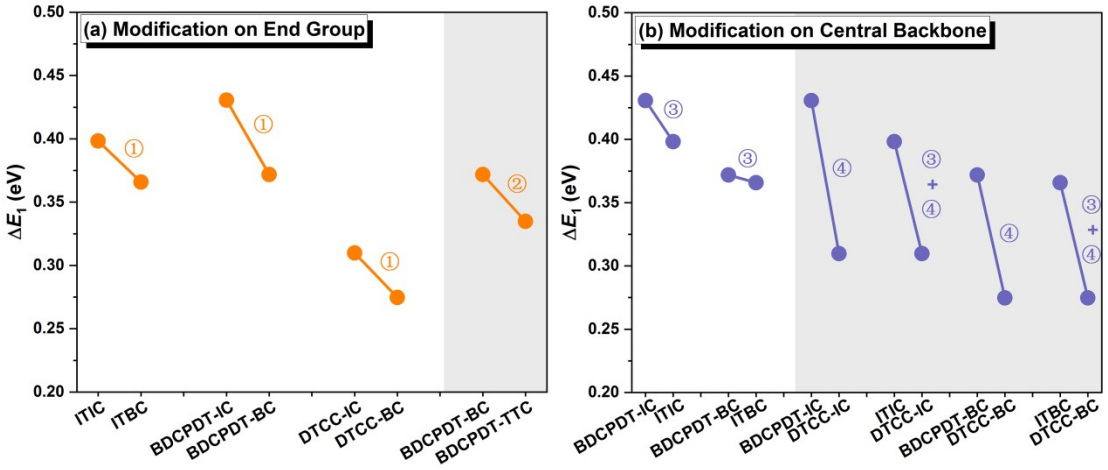

Figure S2. Calculated the energy driving force (ΔE_1, eV) of 10 groups' devices with modification on (a) end group and (b) central backbone of each group, the shadow filling part represents negative correlation.

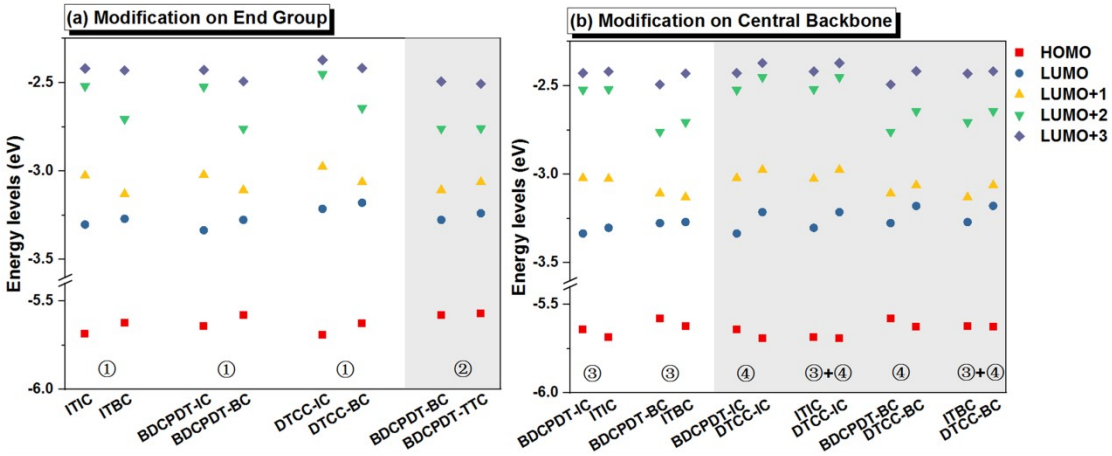

Figure S3. Calculated FMO energy levels (eV) of the optimized acceptors (a) modification on end group and (b) modification on central backbone at PBE0/6-31G(d) levels. The white area indicates positively correlated devices and the dark grey shaded area indicates negatively correlated devices. HOMO and LUMO, while LUMO+1 means the adjacent orbital above it and LUMO+2, LUMO+3.

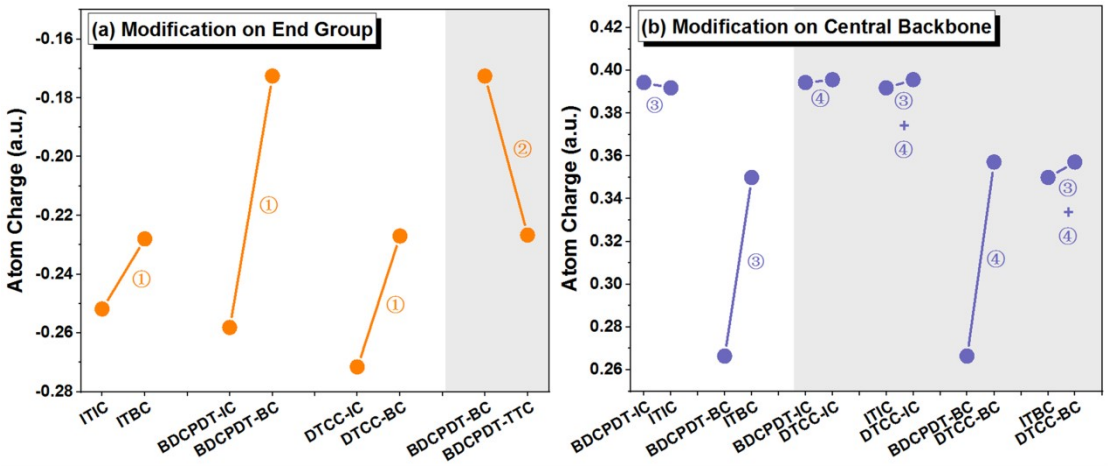

Figure S4. Calculated atomic charges (a.u.) of fragment between NFAs for modification on (a) end groups and (b) central backbones adopted atomic dipole moment corrected Hirshfeld population (ADCH) method at the PBE0/6-31G(d) level. When the atomic charge is positive, it indicates that the group has electron-donating property, it indicates that the electron-donating ability increases following the atomic charge increases. While the atomic charge is negative, the group has electron-withdrawing property, it means the withdrawing electron decreases with the increase of the atomic charge.

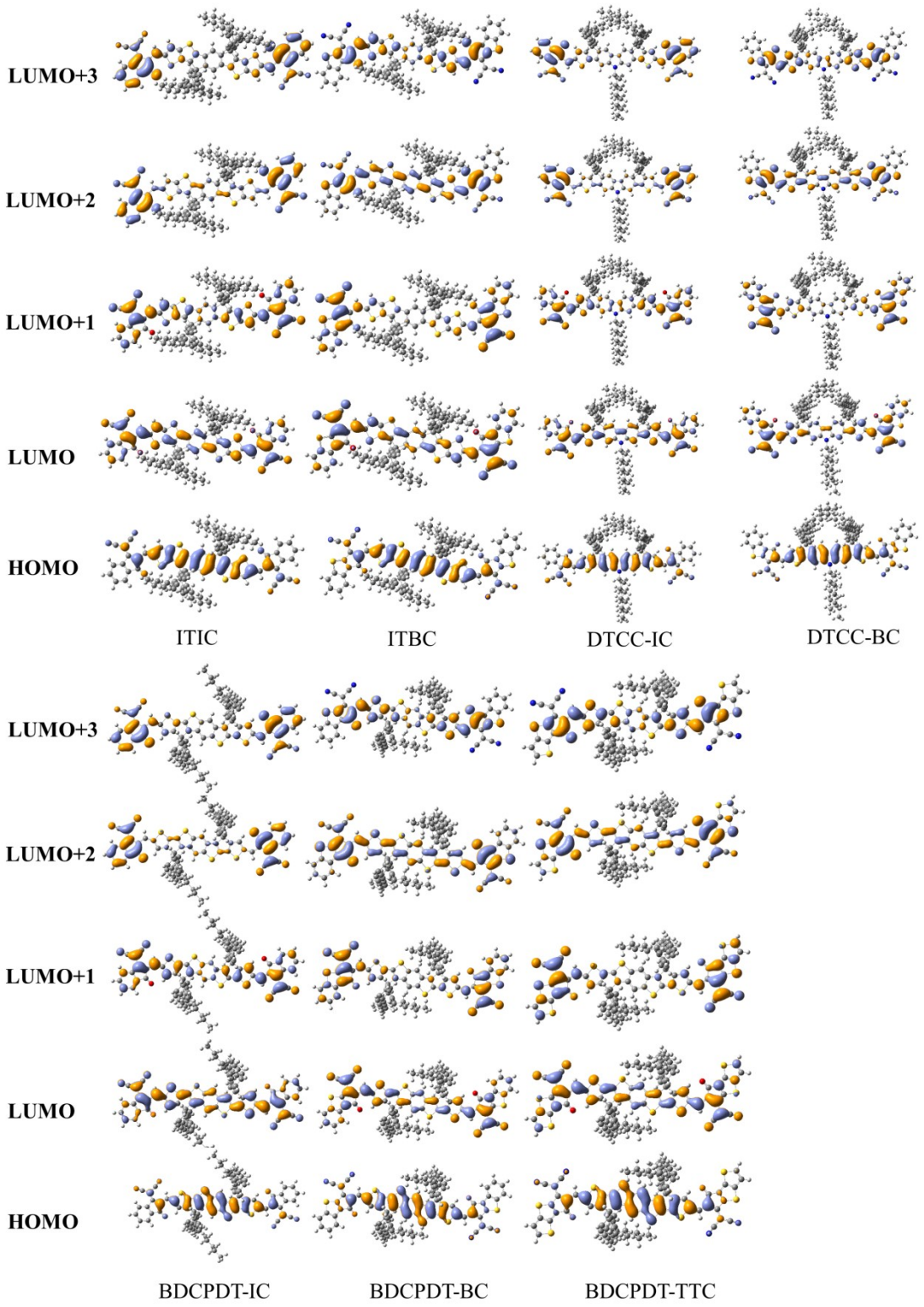

Figure S5. The FMOs of ITIC, ITBC, BDCPDT-IC, BDCPCT-BC, BDCPDT-TTC, DTCC-IC, and DTCC-BC at the PBE0/6-31G(d) level.

Table S1. Fragment modification of molecules of 10 groups with the positive and negative correlation. All acceptor were blended with same donor PBDB-T. Positive represents positive correlation between J_{SC} and V_{OC}, Negative represents negative correlation between J_{SC} and V_{OC}.

Acceptor	Modification	Location	Correlation	Refs.
ITIC→ITBC		end group	Positive	[1,2]
BDCPDT-IC→BDCPDT-BC		end group	Positive	
DTCC-IC→DTCC-BC		end group	Positive	
BDCPDT-BC→BDCPDT-TTC		end group	Negative	
BDCPDT-IC→DTCC-IC	❍	central backbone (D')	Negative	
ITIC→DTCC-IC	●+❍	central backbone (D+D')	Negative	
BDCPDT-BC→DTCC-BC	❍	central backbone (D')	Negative	
ITBC→DTCC-BC	●+❍	central backbone (D+D')	Negative	
BDCPDT-IC→ITIC	●	central backbone	Positive	
BDCPDT-BC→ITBC	●	central backbone	Positive	

 + ; ; ● Extension from inside → outside; ❍ S-configuration→C- configuration.

Table S2. Experiment condition of Yen-Ju Cheng's and Tang's works for ten molecules.[1,2]

	Blend ratio (wt %)	Solvent	Additive
Ref.8	1:1	chlorobenzene	0.5 vol % DIO
Ref.9	1:1	chlorobenzene	0.5 vol % DIO

Table S3. Photovoltaic parameters about J_{SC} (mA cm $^{-2}$), ΔJ_{SC} (mA cm $^{-2}$), V_{OC} (eV) and ΔV_{OC} (eV) with the positive and negative correlation. All acceptor were blended with same donor PBDB-T.

	J_{SC}	ΔJ_{SC}[a]	V_{OC}	ΔV_{OC}[b]	FF	PCE	Refs.
ITIC→ITBC	16.75→19.90	3.15	0.92→0.94	0.02	65.23→64.51	10.05→12.07	[1,2]
BDCPDT-IC→BDCPDT-BC	16.56→18.55	1.99	0.86→0.92	0.06	65.52→63.41	9.33→10.82	
DTCC-IC→DTCC-BC	14.26→17.22	2.96	0.97→0.98	0.01	64.08→63.62	9.25→10.74	
BDCPDT-BC→BDCPDT-TTC	18.55→17.12	-1.43	0.92→0.92	0.00	63.41→61.19	10.82→9.64	
BDCPDT-IC→ITIC	16.56→16.75	0.19	0.86→0.92	0.06	65.52→65.23	9.33→10.05	
BDCPDT-BC→ITBC	18.55→19.90	1.35	0.92→0.94	0.02	63.41→64.51	10.82→12.07	
BDCPDT-IC→DTCC-IC	16.56→14.26	-2.30	0.86→0.97	0.11	65.52→64.08	9.33→9.25	
ITIC→DTCC-IC	16.75→14.26	-2.49	0.92→0.97	0.05	65.23→64.08	10.05→9.25	
BDCPDT-BC→DTCC-BC	18.55→17.22	-1.33	0.92→0.98	0.06	63.41→63.62	10.82→10.74	
ITBC→DTCC-BC	19.90→17.22	-2.68	0.94→0.98	0.04	64.51→63.62	12.07→10.74	

Table S4. Calculated atomic charges (a.u.) of fragment between NFAs adopted atomic dipole moment corrected Hirshfeld population (ADCH) method at the PBE0/6-31G(d) level.

Molecule	Fragment charge	Δ Fragment charge
ITIC	-0.252	0.024
ITBC	-0.228	
BDCPDT-IC	-0.258	0.086
BDCPDT-BC	-0.173	
DTCC-IC	-0.272	0.044
DTCC-BC	-0.227	
BDCPDT-BC	-0.173	-0.054
BDCPDT-TTC	-0.227	
BDCPDT-IC	0.394	-0.002
ITIC	0.392	
BDCPDT-BC	0.266	0.084
ITBC	0.350	
BDCPDT-IC	0.394	0.001
DTCC-IC	0.396	
ITIC	0.392	0.004
DTCC-IC	0.396	
BDCPDT-BC	0.266	0.091
DTCC-BC	0.357	
ITBC	0.350	0.007
DTCC-BC	0.357	

Table S5. Calculated singlet excited energies (eV), oscillator strengths (*f*) and composition of singlet excited states for ITIC-series acceptors at the TD-PBE0/6-31G(d) level. Only the S_2 state of DTCC-IC and DTCC-BC with C-conformation are not forbidden transitions, and HOMO-1 and LUMO+1 participate in the electron jump, respectively. For other S-conformations, the oscillator intensity of the S_2 state in which LUMO+1 participates is 0.

Acceptor	State	Energy (eV)	*f*	Composition
ITIC	S_1	2.018	2.590	H→L (97.9%)
	S_2	2.357	0	H→L+1 (96.6%)
ITBC	S_1	1.953	1.764	H→L (95.3%)
	S_2	2.112	0	H→L+1 (92.8%)
BDCPDT-IC	S_1	1.951	2.487	H→L (98.2%)
	S_2	2.314	0	H→L+1 (95.6%)
BDCPDT-BC	S_1	1.911	1.865	H→L (95.7%)
	S_2	2.089	0	H→L+1 (92.3%)
BDCPDT-TTC	S_1	1.936	1.945	H→L (95.7%)
	S_2	2.121	0	H→L+1 (91.9%)
DTCC-IC	S_1	2.093	2.605	H→L (97.0%)
	S_2	2.352	0.014	H-1→L (95.4%)

DTCC-BC	S_1	2.023	1.724	H→L (93.2%)
	S_2	2.162	0.005	H→L+1 (89.1%)

Table S6. Calculated the HOMO of donor (E^{D}_{HOMO}), LUMO of acceptor (E^{A}_{LUMO}), the stacking distances of donor/acceptor interface model (R) and CT-state energies (E_{CT}) (eV), for donor/ITIC-series acceptors complexes based on $E_{CT} = \left|E^{D}_{HOMO} - E^{A}_{LUMO}\right| - 1/R$.

	E^{D}_{HOMO}	E^{A}_{LUMO}	R	E_{CT}
PBDB-T:ITIC	-5.14	-3.31	3.74	2.08
PBDB-T:ITBC	-5.14	-3.27	3.64	2.15
PBDB-T:BDCPDT-IC	-5.14	-3.36	3.82	2.04
PBDB-T:BDCPDT-BC	-5.14	-3.28	3.87	2.13
PBDB-T:BDCPDT-TTC	-5.14	-3.24	3.92	2.15
PBDB-T:DTCC-IC	-5.14	-3.21	3.75	2.19
PBDB-T:DTCC-BC	-5.14	-3.18	3.74	2.23

Table S7. Experimental energy levels and photovoltaic parameters of devices with positive and negative correlation are used in the machine learning model.

Donor	**Acceptor**	**HOMO**	**LUMO**	**X**	V_{OC}	ΔV_{OC}	J_{SC}	ΔJ_{SC}	**PCE**	**ΔPCE**	**Ref**
Positive correlation											
PBDB-T	BDCPDT-BC	-5.40	-3.85	0.04	0.92	0.02	18.55	1.35	10.82	1.25	[1]
PBDB-T	ITBC	-5.49	-3.90		0.94		19.90		12.07		
PBDB-T	ITIC	-5.61	-4.01	-0.01	0.92	0.02	16.75	3.15	10.05	2.02	[1]
PBDB-T	ITBC	-5.49	-3.9		0.94		19.90		12.07		
PBDB-T	DTCC-IC	-5.47	-3.83	0.01	0.97	0.02	14.26	2.96	9.25	1.49	[1]
PBDB-T	DTCC-BC	-5.46	-3.81		0.98		17.22		10.74		
FTAZ	IDIC1	-5.51	-3.81	0.02	0.90	0.05	13.6	0.7	7.13	2.08	[3]
FTAZ	IHIC1	-5.47	-3.75		0.95		14.3		9.21		
PTB7-Th	F6IC	-5.68	-4.04	-0.2	0.61	0.07	18.15	4.1	7.00	3.7	[4]
PTB7-Th	F8IC1	-5.43	-3.99		0.68		22.25		10.70		
PM6	IT-4F	-5.74	-4.26	-0.03	0.85	0.01	20.02	1.64	12.80	0.61	[5]
PM6	IOM-4F	-5.72	-4.27		0.86		21.66		13.41		
PM6	IOM-4F	-5.72	-4.27	0.05	0.86	0.02	21.66	0.46	13.41	0.76	[5]
PM6	IM-4F	-5.69	-4.19		0.88		22.12		14.17		
PBDB-TF	BDT_iIC-γCl	-5.21	-3.89	-0.04	0.81	0.08	2.26	11.51	6.9	0.71	[6]
PBDB-TF	BDT_cIC-γCl	-5.29	-4.01		0.89		13.77		7.61		
PM6	SiOTC	-5.6	-3.81	-0.06	0.82	0.11	4.92	8.76	1.73	7.13	[7]
PM6	SiOTIC	-5.57	-3.84		0.93		13.68		8.86		
PM6	Z1-aa	-5.67	-3.84	-0.01	0.98	0.02	11.68	3.08	4.56	5.04	[8]

PM6	Z1-ab	-5.69	-3.87		1		14.76		9.6		
PBDB-T	BDCPDT-IC	-5.41	-3.87	0.06	0.86	0.06	16.56	0.19	9.33	0.72	[1]
PBDB-T	ITIC	-5.61	-4.01		0.92		16.75		10.05		
PM6	NOIC3	-5.83	-3.95	-0.14	0.93	0.01	12.9	3.9	7.15	2.95	[9]
PM6	NOIC4	-5.64	-3.9		0.94		16.8		10.1		
PTB7-Th	F6IC	-5.66	-4.02	-0.34	0.61	0.12	18.07	2.76	7.1	3.1	[10]
PTB7-Th	F10IC	-5.26	-3.96		0.73		20.83		10.2		
PTB7-Th	F6IC	-5.66	-4.02	-0.21	0.61	0.03	18.07	7.05	7.1	3.8	[10]
PTB7-Th	F8IC	-5.43	-4		0.64		25.12		10.9		
FTAZ	IHIC2	-5.69	-3.86	-0.2	0.775	0.13	15.7	2.8	7.45	3.75	[11]
FTAZ	IOIC2	-5.41	-3.78		0.902		18.5		11.2		
FTAZ	F5IC	-5.82	-4.05	-0.04	0.70	0.038	14.88	3.55	5.60	2.6	[12]
FTAZ	F7IC	-5.74	-4.01		0.74		18.43		8.20		
FTAZ	F7IC	-5.74	-4.01	-0.18	0.74	0.131	18.43	1.77	8.20	3.5	[12]
FTAZ	F9IC	-5.52	-3.97		0.87		20.20		11.70		
PTB7-Th	F5IC	-5.82	-4.05	-0.2	0.64	0.102	13.89	10.61	5.61	6.29	[13]
PTB7-Th	AOIC	-5.50	-3.93		0.74		24.50		11.90		
PTB7-Th	F8IC1	-5.43	-3.99	-0.05	0.68	0.04	22.25	1.19	10.70	1.6	[4]
PTB7-Th	F10IC1	-5.35	-3.96		0.72		23.44		12.30		
PM6	M8	-5.49	-3.91	0.11	0.83	0.08	8.36	15.27	4.21	11.03	[14]
PM6	M34	-5.6	-3.91		0.91		23.63		15.24		
P3HT	IDBTC	-5.25	-3.54	0.01	0.73	0.02	7.7	1.23	2.5	0.72	[15]
P3HT	IDBTCF	-5.27	-3.55		0.75		8.93		3.22		
PTB7-Th	CO5DFIC	-5.96	-4.29	-0.11	0.59	0.12	12.56	4.76	4.32	1.62	[16]
PTB7-Th	CO5DFIC-OT	-5.51	-3.95		0.71		17.32		5.94		
PTB7-Th	4TIC	-5.36	-4.11	0.10	0.7	0.04	14.58	4.64	5.26	2.87	[17]
PTB7-Th	6TIC	-5.31	-3.96		0.74		19.22		8.13		
PTB7-Th	CO5DFIC	-5.96	-4.29	-0.04	0.59	0.15	12.56	6.67	4.32	4.13	[16]
PTB7-Th	CO5DFIC-ST	-5.55	-3.92		0.74		19.23		8.45		
PTB7-Th	CO5DFIC-OT	-5.51	-3.95	0.07	0.71	0.03	17.32	1.91	5.94	2.51	[16]
PTB7-Th	CO5DFIC-ST	-5.55	-3.92		0.74		19.23		8.45		
PBDB-T	DTNIF	-5.82	-3.92	-0.38	0.9	0.02	13.26	1.23	7.15	1.58	[18]
PBDB-T	DTNSF	-5.52	-4		0.92		14.49		8.73		
PBDB-T	mOEh-ITIC-F	-5.77	-4.23	-0.02	0.68	0.01	13.74	0.45	5.79	-0.01	[19]
PBDB-T	mOEh-ITIC-Cl	-5.74	-4.22		0.69		14.19		5.78		
PBDB-T	mOEh-ITIC-Cl	-5.74	-4.22	0.09	0.68	0.16	12.32	0.01	4.66	1.48	[19]
PBDB-T	mOEh-ITIC	-5.67	-4.06		0.84		12.33		6.14		
J51	ArSiID-F	-5.42	-3.9	-0.01	0.78	0.1	10.4	4	3.1	4.3	[20]
J51	ArSiID	-5.37	-3.86		0.88		14.4		7.4		
J51	ArSiID-Cl	-5.45	-4.01	0.07	0.78	0.1	10	4.4	2.8	4.6	[20]
J51	ArSiID	-5.37	-3.86		0.88		14.4		7.4		
PBDB-T	NTIC-Me	-5.53	-3.73	0.03	0.963	0.002	13.03	0.49	8.3	0.31	[21]

PBDB-T	NTIC-OMe	-5.53	-3.7		0.965		13.52		8.61		
PTB7-Th	T4	-5.36	-4.01	0.16	0.61	0.11	18.57	2.38	7.01	2.81	[22]
PTB7-Th	T1	-5.42	-3.91		0.72		20.95		9.82		
PTB7-Th	T3	-5.31	-4	0.07	0.61	0.06	22	0.65	9.43	0.67	[22]
PTB7-Th	T2	-5.34	-3.96		0.67		22.65		10.1		
PTB7-Th	T4	-5.36	-4.01	0.03	0.61	0.06	18.57	4.07	7.01	3.09	[22]
PTB7-Th	T2	-5.34	-3.96		0.67		22.64		10.1		
PBDB-T	BDCPDT-IC	-5.41	-3.87	0.06	0.86	0.08	16.56	1.16	9.33	0.96	[2]
PBDB-T	BDCPDT-TTC	-5.38	-3.78		0.94		17.72		10.29		
PBDB-T	ITIC	-5.59	-3.91	-0.03	0.87	0.02	15.45	1.26	7.8	2.6	[23]
PBDB-T	IT-OH	-5.57	-3.92		0.89		16.71		10.4		
FTAZ	ITIC-Th	-5.66	-3.93	0.21	0.92	0.047	15.84	0.5	8.90	1.8	[24]
FTAZ	ITIC-Th3	-5.67	-3.73		0.96		16.34		10.70		
PBDB-T	BDCPDT-IC	-5.41	-3.87	0.01	0.86	0.06	16.56	1.99	9.33	1.49	[1]
PBDB-T	BDCPDT-BC	-5.40	-3.85		0.92		18.55		10.82		
PM6	BDSeIC4Br	-5.65	-4.02	0.01	0.86	0.04	16.2	3.8	9.4	2.5	[25]
PM6	BDSeIC2Br	-5.63	-3.99		0.9		20		11.9		
PBDB-T-2F	ITIC-2Br-m	-5.53	-3.9	0.01	0.87	0.02	18.01	1	10.88	1.17	[26]
PBDB-T-2F	ITIC-2Br-γ	-5.54	-3.9		0.89		19.01		12.05		
PBDB-T	ITIC	-5.61	-4.02	0.01	0.9	0.04	16.8	0.64	11.22	0.83	[27]
PBDB-T	IT-M	-5.58	-3.98		0.94		17.44		12.05		
FTAZ	ITIC-Th2	-5.75	-4.07	0.05	0.751	0.098	17.19	2.14	9.06	3.04	[24]
FTAZ	ITIC-Th1	-5.74	-4.01		0.849		19.33		12.1		
PBDB-TF	ITIC-Cl-δ-Th	-5.31	-3.7	0.03	0.89	0.02	17.27	1.03	11.13	1.12	[28]
PBDB-TF	ITIC-Cl-γ-Th	-5.3	-3.66		0.91		18.3		12.25		
J52	i-IEICO-F3	-5.34	-3.74	-0.04	0.897	0.012	16.21	4.69	7.65	5.21	[29]
J52	i-IEICO-2F	-5.29	-3.73		0.909		20.9		12.86		
PBDB-T	BTTIC-0M	-5.62	-3.89	0.01	0.86	0.04	18.95	0.44	11.87	1.28	[30]
PBDB-T	BTTIC-2M	-5.60	-3.86		0.90		19.39		13.15		
PBDB-T	i-mO-4Cl	-5.55	-3.83	-0.03	0.872	0.044	15.08	6.47	7.33	6.52	[31]
PBDB-T	i-mO-4F	-5.5	-3.81		0.916		21.55		13.85		
PCE10	3e	-5.48	-3.65	0.00	0.92	0.09	6.72	2.38	2.52	2.17	[32]
PCE10	3d	-5.42	-3.59		1.01		9.1		4.69		
PBDB-T	IDT-C8-BC	-5.39	-3.5	0.04	1.05	0.03	10.27	0.26	7.3	-1	[33]
PBDB-T	IDT-BC	-5.5	-3.57		1.08		10.53		6.3		
PTB7-Th	IDTP-O-C	-5.47	-3.75	-0.01	0.77	0.02	18.08	0.7	8.61	-0.4	[34]
PTB7-Th	IDTP-P-C	-5.43	-3.72		0.79		18.78		8.21		
FTAZ	ITIC1	-5.48	-3.84	-0.01	0.921	0.025	16.45	1.06	8.54	1.02	[35]
FTAZ	ITIC2	-5.43	-3.8		0.946		17.51		9.56		
PBT1-C	IDTT-C6-TIC	-5.55	-3.99	0.11	0.86	0.04	15.9	1.9	9.5	0.8	[36]
PBT1-C	IDTT-C8-TIC	-5.64	-3.97		0.9		17.8		10.3		
PBDB-T	m-F-ITIC	-5.69	-3.96	-0.01	0.883	0.035	15.8	2.27	8.9	2.21	[37]

PBDB-T	o-F-ITIC	-5.66	-3.94		0.918		18.07		11.11		
PBDB-T	IDTV-ThIC	-5.43	-3.72	-0.03	0.91	0.07	2.06	2.87	0.62	1.15	[38]
PBDB-T	IDTV-PhIC	-5.52	-3.84		0.98		4.93		1.77		
PBDB-T	IDTV-PhIC	-5.52	-3.84	0.17	0.98	0.01	4.93	6.65	1.77	9.81	[38]
PBDB-T	m-IDTV-PhIC	-5.63	-3.78		0.99		11.58		11.58		
PBDB-T-2F	ClBDT-4Cl	-5.72	-3.92	-0.01	0.879	0.009	19.02	0.81	11.65	0.71	[39]
PBDB-T-2F	FBDT-4Cl	-5.7	-3.91		0.888		19.83		12.36		
PBDB-T	IDTCN-S	-5.57	-3.9	0.07	0.85	0.06	19.04	0.92	10.6	2.68	[40]
PBDB-T	IDTCN-O	-5.54	-3.8		0.91		19.96		13.28		
PM6	M38	-5.65	-3.93	-0.08	0.87	0.01	18.28	1.48	8.89	2.27	[41]
PM6	M2	-5.6	-3.96		0.88		19.76		11.16		
PM6	M38	-5.65	-3.93	-0.05	0.87	0.03	18.28	6.35	8.89	7.11	[41]
PM6	M36	-5.62	-3.95		0.9		24.63		16		
PM6	M2	-5.6	-3.96	0.03	0.88	0.02	19.76	4.87	11.16	4.84	[41]
PM6	M36	-5.62	-3.95		0.9		24.63		16		
Negative correlation											
PBDB-T	BDCPDT-BC	-5.40	-3.85	0.05	0.92	0.02	18.55	-0.83	10.82	-0.53	[2]
PBDB-T	BDCPDT-TTC	-5.38	-3.78		0.94		17.72		10.29		
PBDB-T	BDCPDT-IC	-5.41	-3.87	0.10	0.86	0.11	16.56	-2.3	9.33	-0.08	[1]
PBDB-T	DTCC-IC	-5.47	-3.83		0.97		14.26		9.25		
PBDB-T	BDCPDT-BC	-5.40	-3.85	0.10	0.92	0.06	18.55	-1.33	10.82	-0.08	[1]
PBDB-T	DTCC-BC	-5.46	-3.81		0.98		17.22		10.74		
PBDB-T	ITIC	-5.61	-4.01	0.04	0.92	0.05	16.75	-2.49	10.05	-0.8	[1]
PBDB-T	DTCC-IC	-5.47	-3.83		0.97		14.26		9.25		
PBDB-T	ITBC	-5.49	-3.9	0.06	0.94	0.04	19.90	-2.68	12.07	-1.33	[1]
PBDB-T	DTCC-BC	-5.46	-3.81		0.98		17.22		10.74		
PTB7-Th	NOIC	-5.76	-4.03	-0.34	0.885	-0.021	18.1	3.8	11.4	1.1	[9]
PTB7-Th	NOIC1	-5.41	-4.02		0.864		21.9		12.5		
PTB7-Th	NOIC3	-5.83	-3.95	-0.23	0.93	-0.003	12.9	7.7	7.15	6.95	[9]
PTB7-Th	NOIC2	-5.64	-3.99		0.927		20.6		14.1		
PTB7-Th	IEICO	-5.24	-3.8	-0.25	0.88	-0.16	10.7	9.8	6	4.2	[42]
PTB7-Th	IEICO-4F	-5.44	-4.25		0.72		20.5		10.2		
PTB7-Th	FBTIC	-5.7	-3.85	-0.23	0.947	-0.101	14.1	6.5	10.1	2.2	[43]
PTB7-Th	FBDIC	-5.57	-3.95		0.846		20.6		12.3		
PTB7-Th	FNIC1	-5.61	-3.92	-0.13	0.774	-0.033	19.97	3.96	10.3	2.7	[44]
PTB7-Th	FNIC2	-5.56	-4		0.741		23.93		13		
PTB7-Th	AOIC	-5.5	-3.93	-0.11	0.762	-0.018	11.03	13.48	13.7	-9.22	[13]
PTB7-Th	IUIC2	-5.32	-3.86		0.74		24.51		4.48		
PM6	IT-2F	-5.63	-4.06	-0.03	0.92	-0.06	19.3	1.5	12.7	0.9	[45]
PM6	IT-4F	-5.68	-4.14		0.86		20.8		13.6		
PM6	IT-3F	-5.67	-4.09	-0.04	0.9	-0.04	20	0.8	13.8	-0.2	[45]
PM6	IT-4F	-5.68	-4.14		0.86		20.8		13.6		

PM6	ITIC-2Cl	-5.68	-3.99	-0.03	0.92	-0.13	19.1	3.6	10.3	2.9	[46]
PM6	ITIC-4Cl	-5.75	-4.09		0.79		22.7		13.2		
PM6	ITIC-2Cl-β	-5.3	-3.71	-0.07	0.94	-0.06	18.5	0.4	11.2	1	[47]
PM6	α-ITIC-2Cl	-5.29	-3.77		0.88		18.9		12.2		
J71	IT-DM	-5.58	-3.82	-0.12	1.02	-0.11	16.7	1.8	12.1	1.2	[42]
J71	ITCF	-5.59	-3.95		0.91		18.5		13.3		
PBDB-T	IO-4H	-5.61	-3.65	-0.14	1.12	-0.07	5.95	6.25	2.86	5.2	[43]
PBDB-T	IO-4F	-5.65	-3.83		1.05		12.2		8.06		
PBDB-T	IDTTC	-5.4	-3.72	-0.03	1.01	0.02	18.3	-3.8	13.5	-7.04	[48]
PBDB-T	IDTTTC	-5.34	-3.69		1.03		14.5		6.46		
PM6	ITIC-Cl-γ-Th	-5.3	-3.66	-0.07	0.91	-0.05	18.3	0.3	12.3	-0.8	[49]
PM6	ITIC-2Cl-Th	-5.31	-3.74		0.86		18.6		11.5		
PTQ10	m-ITIC-2F	-5.73	-3.95	-0.07	0.96	-0.06	19	0.8	12.5	0	[50]
PTQ10	m-ITIC-4F	-5.73	-4.02		0.9		19.8		12.5		
PM6	POIT-IC2F	-5.6	-3.98	-0.04	0.97	-0.06	18.6	2.3	12.4	1.4	[51]
PM6	POIT-IC4F	-5.65	-4.07		0.91		20.9		13.8		
PTB7-Th	C_6-IDTT-T	-5.71	-3.78	0.09	1.05	0.02	14.4	-1.1	8.51	-0.99	[52]
PTB7-Th	$2C_6$-IDTT-T	-5.74	-3.72		1.07		13.3		7.52		
PM6	C8-ITCC	-5.45	-3.85	-0.03	1.04	-0.09	16.1	1.8	10.8	1.9	[53]
PM6	C8-ITCC-Cl	-5.5	-3.93		0.95		17.9		12.7		
PBT1-C	IDTT-C8-TIC	-5.64	-3.97	0.13	0.88	0.1	20.3	-2.2	13.7	-1	[54]
PBT1-C	IDTT-C10-TIC	-5.71	-3.91		0.98		18.1		12.7		
PTB7-Th	BT-SFIC	-5.46	-4.04	-0.04	0.77	-0.04	18.5	2.8	9.52	0.58	[55]
PTB7-Th	BT-FIC	-5.48	-4.1		0.73		21.3		10.1		
PM6	HBDT-4Cl	-5.67	-3.9	0.03	0.9	-0.02	17.8	1.2	10.4	1.3	[39]
PM6	ClBDT-4Cl	-5.72	-3.92		0.88		19		11.7		
PBDB-T	BTTIC-TT	-5.54	-3.8	-0.04	0.92	0.01	19.6	-3.1	13.4	-4.26	[56]
PBDB-T	BTTIC-Ph	-5.48	-3.78		0.93		16.5		9.14		
PBDB-T	SNBDT1-F	-5.3	-3.83	0.05	0.86	0.02	21	-7.1	12.7	-6.13	[57]
PBDB-T	SNBDT2-F	-5.34	-3.82		0.88		13.9		6.57		
PBDB-T	SNBDT1-F	-5.3	-3.83	0.09	0.86	0.04	21	-8.5	12.7	-6.83	[57]
PBDB-T	SNBDT3-F	-5.36	-3.8		0.9		12.5		5.87		
PBDB-T	SNBDT2-F	-5.34	-3.82	0.04	0.88	0.02	13.9	-1.4	6.57	-0.7	[57]
PBDB-T	SNBDT3-F	-5.36	-3.8		0.9		12.5		5.87		
PBDB-T	IPT2F-Ph	-5.57	-4	0.03	0.86	-0.02	21.2	1	13.1	0.9	[58]
PBDB-T	IPT2F-TT	-5.6	-4		0.84		22.2		14		
PM6	IPTBO-4F	-5.57	-4.07	-0.03	0.92	-0.04	22.1	1.1	14.7	-0.3	[59]
PM6	IPT-4Cl	-5.58	-4.11		0.88		23.2		14.4		
PM6	IN-4F	-5.59	-3.94	-0.13	0.92	-0.09	19.5	1.7	12.5	-1.7	[60]
PM6	IPCl-4F	-5.6	-4.08		0.83		21.2		10.8		
PM6	INO-4F	-5.64	-3.93	-0.19	0.93	-0.1	20.5	0.7	13.7	-2.9	[60]
PM6	IPCl-4F	-5.6	-4.08		0.83		21.2		10.8		

P3HT	l-IDTBTRh	-5.42	-3.68	0.30	0.86	0.06	8.81	-3.81	5.38	-2.85	[61]
P3HT	a-IDTBTRh	-5.63	-3.59		0.92		5		2.53		
J61	BTA1	-5.46	-3.59	0.13	1.24	0.05	5.21	-4.37	3.02	-2.76	[62]
J61	BTA2	-5.43	-3.43		1.29		0.84		0.26		
P3HT	BTA100	-5.32	-3.23	-0.23	1.34	-0.15	1.65	3.68	1.04	2.51	[63]
P3HT	BTA101	-5.41	-3.55		1.19		5.33		3.55		
P3HT	BTA100	-5.32	-3.23	-0.36	1.34	-0.4	1.65	6.91	1.04	4.27	[63]
P3HT	BTA103	-5.37	-3.64		0.94		8.56		5.31		
P3HT	BTA101	-5.41	-3.55	-0.13	1.19	-0.25	5.33	3.23	3.55	1.76	[63]
P3HT	BTA103	-5.37	-3.64		0.94		8.56		5.31		
PM6	NT-4F	-5.88	-3.86	-0.05	0.96	-0.03	13.9	2.7	9.46	1.94	[64]
PM6	NT-4Cl	-5.89	-3.92		0.93		16.6		11.4		
PM6	T-TT-4F	-5.44	-3.51	-0.04	0.86	-0.05	18.5	0.5	10.5	-0.3	[65]
PM6	T-TT-4Cl	-5.48	-3.59		0.81		19		10.2		
PM6	IDT6CN-TM	-5.7	-3.96	-0.08	0.95	-0.09	17.4	0.9	12.4	-1.5	[66]
PM6	IDT6CN-4F	-5.78	-4.12		0.86		18.3		10.9		
PBDB-T	SN61C	-5.38	-3.93	-0.04	0.88	-0.1	16.5	6.7	9.6	3.6	[67]
PBDB-T	SN61C-4F	-5.52	-4.11		0.78		23.2		13.2		
PBDB-T	IXIC	-5.13	-3.78	-0.05	0.82	-0.09	20.9	2.7	11.3	0.9	[68]
PBDB-T	IXIC-2Cl	-5.2	-3.9		0.73		23.6		12.2		
PM6	Z1-ab	-5.69	-3.87	-0.04	1	-0.02	14.8	3.7	9.6	3.1	[8]
PM6	Z1-bb	-5.7	-3.92		0.98		18.5		12.7		
PBT1-C	TTPTTT-IC	-5.64	-3.87	-0.14	1	-0.08	12.5	4.3	7.91	3.59	[69]
PBT1-C	TTPTTT-2F	-5.67	-4.04		0.92		16.8		11.5		
PBT1-C	TTPTTT-2F	-5.67	-4.04	-0.06	0.92	-0.06	16.8	2.6	11.5	0.6	[69]
PBT1-C	TTPTTT-4F	-5.69	-4.12		0.86		19.4		12.1		
PM6	IOIC2	-5.7	-4.16	-0.09	0.97	-0.05	16.3	3.7	10.5	2.3	[70]
PM6	IOIC3	-5.64	-4.19		0.92		20		12.8		
PM6	IOIC3	-5.64	-4.19	0.08	0.92	0.04	20	-2.7	12.8	-1.7	[70]
PM6	IOIC4	-5.7	-4.17		0.96		17.3		11.1		
PM6	IOIC4	-5.7	-4.17	-0.07	0.96	-0.04	17.3	3.6	11.1	2.7	[70]
PM6	IOIC5	-5.65	-4.19		0.92		20.9		13.8		
PM6	IOIC2	-5.7	-4.16	-0.08	0.97	-0.05	16.3	4.6	10.5	3.3	[70]
PM6	IOIC5	-5.65	-4.19		0.92		20.9		13.8		
PM6	NOIC	-5.76	-4.03	-0.34	0.89	-0.03	18.1	3.8	11.4	1.1	[71]
PM6	NOIC1	-5.41	-4.02		0.86		21.9		12.5		
PM6	NOIC1	-5.41	-4.02	0.26	0.86	0.07	21.9	-1.3	12.5	1.6	[71]
PM6	NOIC2	-5.64	-3.99		0.93		20.6		14.1		
PM6	NOIC1	-5.41	-4.02	0.49	0.86	0.07	21.9	-9	12.5	-5.35	[71]
PM6	NOIC3	-5.83	-3.95		0.93		12.9		7.15		
PM6	NOIC	-5.76	-4.03	0.15	0.89	0.04	18.1	-5.2	11.4	-4.25	[71]
PM6	NOIC3	-5.83	-3.95		0.93		12.9		7.15		

PM6	NOIC1	-5.41	-4.02	0.35	0.86	0.08	21.9	-5.1	12.5	-2.4	[71]
PM6	NOIC4	-5.64	-3.9		0.94		16.8		10.1		
PM6	NOIC2	-5.64	-3.99	0.09	0.93	0.01	20.6	-3.8	14.1	-4.0	[71]
PM6	NOIC4	-5.64	-3.9		0.94		16.8		10.1		
J71	ZITI	-5.59	-3.74	0.03	0.93	-0.03	20.4	0.3	13.2	0	[72]
J71	ZITI-3F	-5.64	-3.76		0.9		20.7		13.2		
J71	ZITI-3F	-5.64	-3.76	-0.03	0.9	-0.05	20.7	0.6	13.2	0	[73]
J71	ZITI-4F	-5.66	-3.81		0.85		21.3		13.2		
PBDB-T	FTTCN	-5.54	-3.95	0.03	0.9	0.03	15.9	-0.7	10.6	-0.5	[74]
PBDB-T	FTTCN-M	-5.53	-3.91		0.93		15.2		10.1		

Table S8. Donor/acceptor blending ratio versus the solvent environment for 112 device preparation conditions that achieve positive correlation.

Donor	NFA	D:A ratio	Solvent
FTAZ	IDIC1	1:1.5	$CHCl_3$
FTAZ	IHIC1		
PBDB-TF	BDT_tIC-γCl	1:1.2	chlorobenzene
PBDB-TF	BDT_cIC-γCl		
PM6	SiOTC	1:1.2	chlorobenzene
PM6	SiOTIC		
PM6	Z1-aa	1:1	chlorobenzene
PM6	Z1-ab		
PBDB-T	BDCPDT-IC	1:1	chlorobenzene
PBDB-T	ITIC		
PM6	NOIC3	1:1	chloroform
PM6	NOIC4		
PTB7-Th	F6IC	1:1.7	chloroform
PTB7-Th	F10IC		
PTB7-Th	F6IC	1:1.7	chloroform
PTB7-Th	F8IC		
FTAZ	IHIC2	1:1.5	chloroform
FTAZ	IOIC2		
FTAZ	F5IC	1:1.5	chloroform
FTAZ	F7IC		
FTAZ	F7IC	1:1.5	chloroform
FTAZ	F9IC		
PTB7-Th	F5IC	1:1.5	dichlorobenzene
PTB7-Th	AOIC		
PTB7-Th	F8IC1	1:1.2	chloroform
PTB7-Th	F10IC1		
PM6	M8	1:1	chloroform
PM6	M34		
PTB7-Th	CO5DFIC	1:1	chlorobenzene
PTB7-Th	CO5DFIC-OT		
PTB7-Th	4TIC	1:1.3	chloroform
PTB7-Th	6TIC		
PBDB-T	DTNIF	1:1	chlorobenzene
PBDB-T	DTNSF		
PBDB-T	mOEh-ITIC-F	1:1	chlorobenzene
PBDB-T	mOEh-ITIC-Cl		
PBDB-T	mOEh-ITIC-Cl	1:1	Xylene
PBDB-T	mOEh-ITIC		
J51	ArSiID-F	1:1	chloroform
J51	ArSiID		

J51	ArSiID-Cl	1:1	chloroform
J51	ArSiID		
PBDB-T	NTIC-Me	1：0.8	chloroform
PBDB-T	NTIC-OMe		
PTB7-Th	T4	1:1.8	chlorobenzene
PTB7-Th	T1		
PTB7-Th	T3	1:1.8	chlorobenzene
PTB7-Th	T2		
PTB7-Th	T4	1:1.8	chlorobenzene
PTB7-Th	T2		
PBDB-T	ITIC	1:1	chlorobenzene
PBDB-T	IT-OH		
FTAZ	ITIC-Th	1:1.5	chloroform
FTAZ	ITIC-Th3		
PBDB-T	BDCPDT-IC	1:1	chlorobenzene
PBDB-T	BDCPDT-BC		
PM6	BDSeIC4Br	1:1	chlorobenzene
PM6	BDSeIC2Br		
PBDB-T-2F	ITIC-2Br-m	1:1	chlorobenzene
PBDB-T-2F	ITIC-2Br-γ		
PBDB-T	ITIC	1:1	chlorobenzene
PBDB-T	IT-M		
FTAZ	ITIC-Th2	1:1.5	chloroform
FTAZ	ITIC-Th1		
PBDB-TF	ITIC-Cl-δ-Th	1:1	chlorobenzene
PBDB-TF	ITIC-Cl-γ-Th		
J52	i-IEICO-F3	1:1	chlorobenzene
J52	i-IEICO-2F		
PBDB-T	i-mO-4Cl	1:1	chlorobenzene
PBDB-T	i-mO-4F		
PBDB-T	IDT-C8-BC	1:1.5	chlorobenzene
PBDB-T	IDT-BC		
PTB7-Th	IDTP-O-C	1:1	chloroform
PTB7-Th	IDTP-P-C		
FTAZ	ITIC1	1:1.3	chloroform
FTAZ	ITIC2		
PBT1-C	IDTT-C6-TIC	1:1.3	chloroform
PBT1-C	IDTT-C8-TIC		
PBDB-T	m-F-ITIC	1.3:1	chlorobenzene
PBDB-T	o-F-ITIC		
PBDB-T	IDTV-ThIC	1:1	chlorobenzene
PBDB-T	IDTV-PhIC		
PBDB-T	IDTV-PhIC	1:1	chlorobenzene
PBDB-T	m-IDTV-PhIC		

PBDB-T-2F	ClBDT-4Cl	1:1	chlorobenzene
PBDB-T-2F	FBDT-4Cl		
PBDB-T	IDTCN-S	1:1	1,2-dichlorobenzene
PBDB-T	IDTCN-O		
PM6	M38	1:1	chloroform
PM6	M2		
PM6	M38	1:1	chloroform
PM6	M36		
PM6	M2	1:1	chloroform
PM6	M36		

II. Calculation Methods

Since PBE0 method could provide an accurate evaluation of geometric and electronic structures for thiophene derivatives.[75-76] The ground geometrical configurations were optimized by density functional theory (DFT) with the PBE0 functional and 6-31G(d) basis set (**Fig. S1**). For the quantum chemical study of molecular systems, the ADCH method shows good reproducibility in terms of charge rationality, basis set dependence, *etc*.[77] Thereby, the atom charges of fragment were calculated adopted ADCH method in Multiwfn 3.8.[78] All calculations were carried out by using the Gaussian 09 package.[79]

III. Machine learning model: prediction of positive and negative correlation

```
import numpy as np
import matplotlib.pyplot as plt
import pandas as pd
from pandas import read_csv
import scipy
train_set = read_csv('train.csv', dtype = np.float32)
test_set = read_csv('test.csv', dtype = np.float32)
train_data_orig = train_set.values
test_data_orig = test_set.values
train_x = train_data_orig [:, 1:]
train_set_x = train_x .reshape(train_x .shape[0], -1).T
train_set_y = train_data_orig[:, 0]
test_x = test_data_orig[:, 1:]
test_set_x = test_x .reshape(test_x .shape[0], -1).T
test_set_y = test_data_orig[:, 0]
def sigmod(z):
    s = 1/(1+np.exp(-z))
return s
def initialize_with_zeros(dim):
    w = np.zeros((dim, 1))
    b = 0
    return w, b
def propagate(w, b, X, Y):
    m = X.shape[1]
```

```
        Z = np.dot(w.T, X)+b
        A = sigmod(Z)
        cost = (-(np.dot(Y, np.log(A).T)+np.dot((1-Y), np.log(1-A).T)))/m
        db = np.sum(A-Y)/m
        dw = np.dot(X, (A-Y).T)/m
        grads = {'dw':dw, 'db':db}
    return grads, cost
    def optimize(w, b, X, Y, num_iterations, learning_rate):
        costs = []
        for i in range(num_iterations):
            grads, cost = propagate(w, b, X, Y)
            dw = grads['dw']
            db = grads['db']
            w = w-learning_rate*dw
            b = b-learning_rate*db
            if i%100 == 0:
                np.squeeze(cost)
                costs.append(cost)

        params = {'w':w, "b":b}

    return params, costs
    def prediciton(w, b, X):
        m = X.shape[1]
        Y_pred = np.zeros((1, m))
        w = w.reshape(X.shape[0], 1)
        A = sigmod(np.dot(w.T, X)+b)
        for i in range(A.shape[1]):
            if A[0][i]< = 0.5:
                A[0][i] = 0
            else:
                A[0][i] = 1
        Y_pred = A
    return Y_pred
    def model(X_train, X_test, Y_train, Y_test,num_iterations = 60000, learning_rate = 0.01):
        w, b = initialize_with_zeros(X_train.shape[0])
        parameters, costs = optimize(w, b, X_train, Y_train, num_iterations, learning_rate)
        w = parameters["w"]
        b = parameters["b"]
        Y_prediction_test = prediciton(w, b, X_test)
        Y_prediction_train = prediciton(w, b, X_train)
        print('train accuracy: {}%'.format(100-np.mean(np.abs(Y_prediction_train-Y_train))*100))
        print('test accuracy: {}%'.format(100-np.mean(np.abs(Y_prediction_test-Y_test))*100))
        d = {'costs':costs,
```

```
        'Y_prediction_test':Y_prediction_test,
        'Y_prediction_train':Y_prediction_train,
        "w":w,
        "b":b,
        'learning_rate':learning_rate,
        "num_iterations":num_iterations}
    print("y = {}x+{}".format(d["w"], d["b"]))
return d

d = model(train_set_x, test_set_x, train_set_y, test_set_y, num_iterations = 60000, learning_rate = 0.01)
costs = np.squeeze(d['costs'])
```

IV. Appendix Full Name

Full Name	Abbreviation
3,9-bis(2-methylene-(3-(1,1-dicyanomethylene)-in-danone)-5,5,11,11-tetrakis(4-hexyl-phenyl)-dithieno[2,3-d:2',3'-d']-s-inndaceno[1,2-b:5,6-b'] dithiophene	ITIC
C6-olefinated2-(3-oxo-2,3-dihydro-1H-benzo[b]cyclopenta[d]thiophen-1-ylidene)-malononitrile with two 2-(3-oxo-2,3-dihydro-1H-benzo[b]cyclopenta[d] thiophen-1-ylidene)-malononitrile (BC) moieties	ITBC
Thieno[3,2-b]thiophene (BDCPDT) with two 1,1-dicyanomethylene-3-indanone (IC) moieties	BDCPDT-IC
Thieno[3,2-b]thiophene with two 2-(3-oxo-2,3-dihydro-1H-benzo[b]cyclopenta[d] thiophen-1-ylidene)-malononitrile (BC) moieties	BDCPDT-BC
Thieno[3,2-b]thiophene with two 2-(5-oxo-5,6-dihydro-7H-cyclopenta[b]thieno [2,3-d]thiophen-7-ylidene)malononitrile (TTC) moieties	BDCPDT-TTC
dithienocyclopentacarbazole (DTCC) with two 1,1-dicyanomethylene-3-indanone (IC) moieties	DTCC-IC
dithienocyclopentacarbazole (DTCC) with two 2-(3-oxo-2,3-dihydro-1H-benzo[b]cyclopenta[d] thiophen-1-ylidene)-malononitrile (BC) moieties	DTCC-BC
poly[(2,6-(4,8-bis(5-(2-ethylhexyl)thiophen-2-yl)-benzo[1,2-b:4,5-b']dithiophene))-alt-(5,5-(1',3'-di2-thienyl-5',7'-bis(2-ethylhexyl)benzo[1',2'-c:4',5'-']dithiophene-4,8-dione))])	PBDB-T

V. References

(1) Chang, S.-L.; Hung, K.-E.; Cao, F.-Y.; Huang, K.-H.; Hsu, C.-S.; Liao, C.-Y.; Lee, C.-H.; Cheng, Y.-J., Isomerically Pure Benzothiophene-Incorporated Acceptor: Achieving Improved Voc and Jsc of Nonfullerene Organic Solar Cells via End Group Manipulation. ACS Applied Materials & Interfaces 2019, 11, 33179-33187.

(2) Chang, S.-L.; Cao, F.-Y.; Huang, W.-C.; Huang, P.-K.; Huang, K.-H.; Hsu, C.-S.; Cheng, Y.-J., New Thieno[3,2-b]thiophene-Based Acceptor: Tuning Acceptor Strength of Ladder-Type N-Type Materials to Simultaneously Achieve Enhanced Voc and Jsc of Nonfullerene Solar Cells. ACS Energy Letters 2018, 3, 1722-1729.

(3) Zhu, J.; Wu, Y.; Rech, J.; Wang, J.; Liu, K.; Li, T.; Lin, Y.; Ma, W.; You, W.; Zhan, X., Enhancing the performance of a fused-ring electron acceptor via extending benzene to naphthalene.

Journal of Materials Chemistry C 2018, 6, 66-71.
(4) Wang, W.; Lu, H.; Chen, Z.; Jia, B.; Li, K.; Ma, W.; Zhan, X., High-performance NIR-sensitive fused tetrathienoacene electron acceptors. Journal of Materials Chemistry A 2020, 8, 3011-3017.
(5) Zhang, Z.; Wang, H.; Yu, J.; Sun, R.; Xu, J.; Yang, L.; Geng, R.; Cao, J.; Du, F.; Min, J.; Liu, F.; Tang, W., Modification on the Indacenodithieno[3,2-b]thiophene Core to Achieve Higher Current and Reduced Energy Loss for Nonfullerene Solar Cells. Chemistry of Materials 2020, 32, 1297-1307.
(6) Lai, H.; Guo, M.; Zhu, Y.; Chen, L.; Tan, P.; Yang, C.; He, F., The cis- and trans-orientation of benzo[1,2-b:4,5-b′]dithiophene-based isomers in organic solar cells. Materials Chemistry Frontiers 2021, 5, 1486-1494.
(7) Qin, Y.; Chen, H.; Yao, J.; Zhou, Y.; Cho, Y.; Zhu, Y.; Qiu, B.; Ju, C. W.; Zhang, Z. G.; He, F.; Yang, C.; Li, Y.; Zhao, D., Silicon and oxygen synergistic effects for the discovery of new high-performance nonfullerene acceptors. Nat Commun 2020, 11, 5814.
(8) Zhou, Z.; Duan, J.; Ye, L.; Wang, G.; Zhao, B.; Tan, S.; Shen, P.; Ryu, H. S.; Woo, H. Y.; Sun, Y., Simultaneously improving the photovoltaic parameters of organic solar cells via isomerization of benzo[b]benzo[4,5]thieno[2,3-d]thiophene-based octacyclic non-fullerene acceptors. Journal of Materials Chemistry A 2020, 8, 9684-9692.
(9) Li, T.; Wu, Y.; Zhou, J.; Li, M.; Wu, J.; Hu, Q.; Jia, B.; Pan, X.; Zhang, M.; Tang, Z.; Xie, Z.; Russell, T. P.; Zhan, X., Butterfly Effects Arising from Starting Materials in Fused-Ring Electron Acceptors. J Am Chem Soc 2020, 142, 20124-20133.
(10) Dai, S.; Li, T.; Wang, W.; Xiao, Y.; Lau, T.-K.; Li, Z.; Liu, K.; Lu, X.; Zhan, X., Enhancing the Performance of Polymer Solar Cells via Core Engineering of NIR-Absorbing Electron Acceptors. Advanced Materials 2018, 30, 1706571.
(11) Zhu, J.; Ke, Z.; Zhang, Q.; Wang, J.; Dai, S.; Wu, Y.; Xu, Y.; Lin, Y.; Ma, W.; You, W.; Zhan, X., Naphthodithiophene-Based Nonfullerene Acceptor for High-Performance Organic Photovoltaics: Effect of Extended Conjugation. Adv Mater 2018, 30.
(12) Dai, S.; Xiao, Y.; Xue, P.; James Rech, J.; Liu, K.; Li, Z.; Lu, X.; You, W.; Zhan, X., Effect of Core Size on Performance of Fused-Ring Electron Acceptors. Chemistry of Materials 2018, 30, 5390-5396.
(13) Jia, B.; Wang, J.; Wu, Y.; Zhang, M.; Jiang, Y.; Tang, Z.; Russell, T. P.; Zhan, X., Enhancing the Performance of a Fused-Ring Electron Acceptor by Unidirectional Extension. Journal of the American Chemical Society 2019, 141, 19023-19031.
(14) Ma, Y.; Cai, D.; Wan, S.; Wang, P.; Wang, J.; Zheng, Q., Ladder-Type Heteroheptacenes with Different Heterocycles for Nonfullerene Acceptors. Angew Chem Int Ed Engl 2020, 59, 21627-21633.
(15) He, A.; Qin, Y.; Zhou, D.; Ni, C., Effective design of novel low band gap acceptors for non-fullerene solar cells via modulating molecular planarity and F atom substitution. Materials Letters 2020, 258, 126785.
(16) Zhang, L.; Jin, K.; Xiao, Z.; Wang, X.; Wang, T.; Yi, C.; Ding, L., Alkoxythiophene and alkylthiothiophene π-bridges enhance the performance of A–D–A electron acceptors. Materials Chemistry Frontiers 2019, 3, 492-495.
(17) Zhang, Z.; Shan, T.; Zhang, Y.; Zhu, L.; Kong, L.; Liu, F.; Zhong, H., Isomerizing thieno[3,4-b]thiophene-based near-infrared non-fullerene acceptors towards efficient organic solar cells. Journal of Materials Chemistry C 2020, 8, 4357-4364.
(18) Zhang, M.; Ma, Y.; Zheng, Q., Dithienonaphthalene-Based Non-fullerene Acceptors With Different Bandgaps for Organic Solar Cells. Front Chem 2018, 6, 427.

(19) Sung, M. j.; Park, B.; Choi, J. Y.; Kim, J.; Sun, C.; Kang, H.; Kwon, S.; Jang, S.-Y.; Kim, Y.-H.; Lee, K.; Kwon, S.-K., Spirobifluorene-based non-fullerene acceptors for the environmentally benign process. Dyes and Pigments 2020, 180, 108369.

(20) Wang, C. K.; Jiang, B. H.; Su, Y. W.; Jeng, R. J.; Wang, Y. J.; Chen, C. P.; Wong, K. T., Si-Bridged Ladder-Type Small-Molecule Acceptors for High-Performance Organic Photovoltaics. ACS Appl Mater Interfaces 2019, 11, 1125-1134.

(21) Yi, Y.-Q.-Q.; Feng, H.; Chang, M.; Zhang, H.; Wan, X.; Li, C.; Chen, Y., New small-molecule acceptors based on hexacyclic naphthalene(cyclopentadithiophene) for efficient non-fullerene organic solar cells. Journal of Materials Chemistry A 2017, 5, 17204-17210.

(22) Chen, F. X.; Xu, J. Q.; Liu, Z. X.; Chen, M.; Xia, R.; Yang, Y.; Lau, T. K.; Zhang, Y.; Lu, X.; Yip, H. L.; Jen, A. K.; Chen, H.; Li, C. Z., Near-Infrared Electron Acceptors with Fluorinated Regioisomeric Backbone for Highly Efficient Polymer Solar Cells. Adv Mater 2018, 30, e1803769.

(23) Liu, X.; Wang, X.; Xiao, Y.; Yang, Q.; Guo, X.; Li, C., H‐Bonds‐Assisted Molecular Order Manipulation of Nonfullerene Acceptors for Efficient Nonannealed Organic Solar Cells. Advanced Energy Materials 2020, 10, 1903650.

(24) Li, Z.; Dai, S.; Xin, J.; Zhang, L.; Wu, Y.; Rech, J.; Zhao, F.; Li, T.; Liu, K.; Liu, Q.; Ma, W.; You, W.; Wang, C.; Zhan, X., Enhancing the performance of the electron acceptor ITIC-Th via tailoring its end groups. Materials Chemistry Frontiers 2018, 2, 537-543.

(25) Wan, S. S.; Chang, C.; Wang, J. L.; Yuan, G. Z.; Wu, Q.; Zhang, M.; Li, Y., Effects of the Number of Bromine Substitution on Photovoltaic Efficiency and Energy Loss of Benzo[1,2‐b:4,5‐b′]diselenophene‐based Narrow‐Bandgap Multibrominated Nonfullerene Acceptors. Solar RRL 2018, 1800250.

(26) Qu, J.; Li, D.; Wang, H.; Zhou, J.; Zheng, N.; Lai, H.; Liu, T.; Xie, Z.; He, F., Bromination of the Small-Molecule Acceptor with Fixed Position for High-Performance Solar Cells. Chemistry of Materials 2019, 31, 8044-8051.

(27) Li, S.; Ye, L.; Zhao, W.; Zhang, S.; Mukherjee, S.; Ade, H.; Hou, J., Energy-Level Modulation of Small-Molecule Electron Acceptors to Achieve over 12% Efficiency in Polymer Solar Cells. Adv Mater 2016, 28, 9423-9429.

(28) Lai, H.; Chen, H.; Shen, Y.; Wang, M.; Chao, P.; Xie, W.; Qu, J.; Yang, B.; He, F., Using Chlorine Atoms to Fine-Tune the Intermolecular Packing and Energy Levels of Efficient Nonfullerene Acceptors. ACS Applied Energy Materials 2019, 2, 7663-7669.

(29) Wu, H.; Zhao, B.; Zhao, H.; Wang, L.; Wang, W.; Cong, Z.; Liu, J.; Ma, W.; Gao, C., Effects of Monofluorinated Positions at the End-Capping Groups on the Performances of Twisted Non-Fullerene Acceptor-Based Polymer Solar Cells. ACS Appl Mater Interfaces 2020, 12, 789-797.

(30) Gao, W.; Liu, T.; Luo, Z.; Zhang, L.; Ming, R.; Zhong, C.; Ma, W.; Yan, H.; Yang, C., Regulating exciton bonding energy and bulk heterojunction morphology in organic solar cells via methyl-functionalized non-fullerene acceptors. Journal of Materials Chemistry A 2019, 7, 6809-6817.

(31) Zhao, B.; Wang, W.; Xie, Y.; Zhao, H.; Wang, L.; Liu, S.; Xin, J.; Cong, Z.; Wu, H.; Liang, Q.; Ma, W.; Gao, C.; Wu, H.; Cao, Y., Efficient Polymer Solar Cells Enabled by Alkoxy-Phenyl Side-Chain-Modified Main-Chain-Twisted Small Molecular Acceptors. Journal of Materials Chemistry A 2020, 8, 22335-22345.

(32) Xiao, L.; Kolaczkowski, M. A.; Min, Y.; Liu, Y., Substitution Effect on Thiobarbituric Acid End Groups for High Open-Circuit Voltage Non-Fullerene Organic Solar Cells. ACS Appl Mater Interfaces 2020, 12, 41852-41860.

(33) Zhang, J.; Lv, J.; Dong, X.; Xu, T.; Dai, X.; Duan, T.; Kan, Z.; Liu, P.; Lu, S., Cyano-functionalized small-molecule acceptors for high-efficiency wide-bandgap organic solar cells. Journal of Materials Chemistry C 2020, 8, 9195-9200.

(34) Pang, Z.; Zhang, W.; Wu, J.; Luo, Y.; Liu, J.; Zhao, S.; Xu, Z.; Lu, Z.; Huang, Y., Insight into the effects of alkoxy side chain position in nonfullerene electron acceptors on the morphological stability of organic solar cells. Dyes and Pigments 2020, 181, 108562.

(35) Wang, J.; Wang, W.; Wang, X.; Wu, Y.; Zhang, Q.; Yan, C.; Ma, W.; You, W.; Zhan, X., Enhancing Performance of Nonfullerene Acceptors via Side-Chain Conjugation Strategy. Adv Mater 2017, 29.

(36) Ye, L.; Weng, K.; Xu, J.; Du, X.; Chandrabose, S.; Chen, K.; Zhou, J.; Han, G.; Tan, S.; Xie, Z.; Yi, Y.; Li, N.; Liu, F.; Hodgkiss, J. M.; Brabec, C. J.; Sun, Y., Unraveling the influence of non-fullerene acceptor molecular packing on photovoltaic performance of organic solar cells. Nat Commun 2020, 11, 6005.

(37) Lee, J.; Go, E. M.; Dharmapurikar, S.; Xu, J.; Lee, S. M.; Jeong, M.; Lee, K. C.; Oh, J.; Cho, Y.; Zhang, C.; Xiao, M.; Kwak, S. K.; Yang, C., Insights into constitutional isomeric effects on donor–acceptor intermolecular arrangements in non-fullerene organic solar cells. Journal of Materials Chemistry A 2019, 7, 18468-18479.

(38) Liang, J.; Yin, P.; Zheng, T.; Wang, G.; Zeng, X.; Cui, C.; Shen, P., Conjugated side-chain optimization of indacenodithiophene-based nonfullerene acceptors for efficient polymer solar cells. Journal of Materials Chemistry C 2019, 7, 10028-10038.

(39) Yuan, G.-Z.; Fan, H.; Wan, S.-S.; Jiang, Z.; Liu, Y.-Q.; Liu, K.-K.; Bai, H.-R.; Zhu, X.; Wang, J.-L., A two-dimensional halogenated thiophene side-chain strategy for balancing Voc and Jsc and improving efficiency of non-fullerene small molecule acceptor-based organic solar cells. Journal of Materials Chemistry A 2019, 7, 20274-20284.

(40) Liu, Y.; Li, M.; Yang, J.; Xue, W.; Feng, S.; Song, J.; Tang, Z.; Ma, W.; Bo, Z., High‐Efficiency As‐Cast Organic Solar Cells Based on Acceptors with Steric Hindrance Induced Planar Terminal Group. Advanced Energy Materials 2019, 9, 1901280.

(41) Ma, Y.; Cai, D.; Wan, S.; Yin, P.; Wang, P.; Lin, W.; Zheng, Q., Control over π-π stacking of heteroheptacene-based nonfullerene acceptors for 16% efficiency polymer solar cells. National Science Review 2020, 7, 1886-1895.

(42) Hao, M.; Liu, T.; Xiao, Y.; Ma, L.-K.; Zhang, G.; Zhong, C.; Chen, Z.; Luo, Z.; Lu, X.; Yan, H.; Wang, L.; Yang, C., Achieving Balanced Charge Transport and Favorable Blend Morphology in Non-Fullerene Solar Cells via Acceptor End Group Modification. Chemistry of Materials 2019, 31, 1752-1760.

(43) Xian, K.; Cui, Y.; Xu, Y.; Zhang, T.; Hong, L.; Yao, H.; An, C.; Hou, J., Efficient Exciton Dissociation Enabled by the End Group Modification in Non-Fullerene Acceptors. The Journal of Physical Chemistry C 2020.

(44) Wang, J.; Zhang, J.; Xiao, Y.; Xiao, T.; Zhu, R.; Yan, C.; Fu, Y.; Lu, G.; Lu, X.; Marder, S. R.; Zhan, X., Effect of Isomerization on High-Performance Nonfullerene Electron Acceptors. Journal of the American Chemical Society 2018, 140, 9140-9147.

(45) Gao, B.; Yao, H.; Hou, J.; Yu, R.; Hong, L.; Xu, Y.; Hou, J., Multi-component non-fullerene acceptors with tunable bandgap structures for efficient organic solar cells. Journal of Materials Chemistry A 2018, 6, 23644-23649.

(46) Zhang, H.; Yao, H.; Hou, J.; Zhu, J.; Zhang, J.; Li, W.; Yu, R.; Gao, B.; Zhang, S.; Hou, J., Over

14% Efficiency in Organic Solar Cells Enabled by Chlorinated Nonfullerene Small-Molecule Acceptors. Advanced Materials 2018, 30, 1800613.

(47) Lai, H.; Chen, H.; Zhou, J.; Qu, J.; Wang, M.; Xie, W.; Xie, Z.; He, F., 3D Interpenetrating Network for High-Performance Nonfullerene Acceptors via Asymmetric Chlorine Substitution. The Journal of Physical Chemistry Letters 2019, 10.

(48) Deng, M.; Xu, X.; Lee, Y. W.; Ericsson, L. K. E.; Moons, E.; Woo, H. Y.; Li, Y.; Yu, L.; Peng, Q., Fine regulation of crystallisation tendency to optimize the BHJ nanostructure and performance of polymer solar cells. Nanoscale 2020, 12, 12928-12941.

(49) Lai, H.; Chen, H.; Shen, Y.; Wang, M.; Chao, P.; Xie, W.; Qu, J.; Yang, B.; He, F., Using Chlorine Atoms to Fine-Tune the Intermolecular Packing and Energy Levels of Efficient Nonfullerene Acceptors. ACS Applied Energy Materials 2019, 2019.

(50) Li, X.; Yao, J.; Angunawela, I.; Sun, C.; Xue, L.; Liebman-Pelaez, A.; Zhu, C.; Yang, C.; Zhang, Z.-G.; Ade, H.; Li, Y., Improvement of Photovoltaic Performance of Polymer Solar Cells by Rational Molecular Optimization of Organic Molecule Acceptors. Advanced Energy Materials 2018, 8, 1800815.

(51) Fan, Q.; Su, W.; Zhang, M.; Wu, J.; Jiang, Y.; Guo, X.; Liu, F.; Russell, T. P.; Zhang, M.; Li, Y., Synergistic Effects of Side-Chain Engineering and Fluorination on Small Molecule Acceptors to Simultaneously Broaden Spectral Response and Minimize Voltage Loss for 13.8% Efficiency Organic Solar Cells. Solar RRL 2019, 3, 1900169.

(52) Xia, T.; Li, C.; Ryu, H. S.; Sun, X.; Woo, H. Y.; Sun, Y., Asymmetrically Alkyl-Substituted Wide-Bandgap Nonfullerene Acceptor for Organic Solar Cells. Solar RRL 2020, 4, 2000061.

(53) Zhang, J.; Li, Y.; Hu, H.; Zhang, G.; Ade, H.; Yan, H., Chlorinated Thiophene End Groups for Highly Crystalline Alkylated Non-Fullerene Acceptors toward Efficient Organic Solar Cells. Chemistry of Materials 2019, 31, 6672-6676.

(54) Ye, L.; Weng, K.; Xu, J.; Du, X.; Chandrabose, S.; Chen, K.; Zhou, J.; Han, G.; Tan, S.; Xie, Z.; Yi, Y.; Li, N.; Liu, F.; Hodgkiss, J. M.; Brabec, C. J.; Sun, Y., Unraveling the influence of non-fullerene acceptor molecular packing on photovoltaic performance of organic solar cells. Nature Communications 2020, 11, 6005.

(55) Li, Y.; Su, W.; Wu, F.; Xu, Z.; Wang, Y.-K.; Zhang, M.; Jiang, Z.-Q.; Liao, L.-S., Near-infrared non-fullerene acceptors based on dithienyl[1,2-b:4,5-b']benzodithiophene core for high performance PTB7-Th-based polymer solar cells. Organic Electronics 2019, 65, 63-69.

(56) Liu, T.; Gao, W.; Wang, Y.; Yang, T.; Ma, R.; Zhang, G.; Zhong, C.; Ma, W.; Yan, H.; Yang, C., Unconjugated Side-Chain Engineering Enables Small Molecular Acceptors for Highly Efficient Non-Fullerene Organic Solar Cells: Insights into the Fine-Tuning of Acceptor Properties and Micromorphology. Advanced Functional Materials 2019, 29, 1902155.

(57) Zeng, G.; Xin, Y.; Zhang, B.; Ouyang, J.; Zhao, X.; Yang, X., Significantly Increasing the Power Conversion Efficiency by Controlling the Orientation of Nonfullerene Small Molecular Acceptors via Side Chain Engineering. Solar RRL 2020, 4, 2000234.

(58) Cao, J.; Wang, H.; Qu, S.; Yu, J.; Yang, L.; Zhang, Z.; Du, F.; Tang, W., 2D Side-Chain Engineered Asymmetric Acceptors Enabling Over 14% Efficiency and 75% Fill Factor Stable Organic Solar Cells. Advanced Functional Materials 2020, 30, 2006141.

(59) Yang, L.; Hu, Z.; Zhang, Z.; Cao, J.; Wang, H.; Yu, J.; Zhang, F.; Tang, W., Molecular engineering of acceptors to control aggregation for optimized nonfullerene solar cells. Journal of Materials Chemistry A 2020, 8, 5458-5466.

(60) Zhang, Z.; Yang, L.; Hu, Z.; Yu, J.; Liu, X.; Wang, H.; Cao, J.; Zhang, F.; Tang, W., Charge

density modulation on asymmetric fused-ring acceptors for high-efficiency photovoltaic solar cells. Materials Chemistry Frontiers 2020, 4, 1747-1755.

(61) Huang, H.; Xiao, B.; Huang, C.; Zhang, J.; Liu, S.; Fu, N.; Zhao, B.; Qin, T.; Zhou, E.; Huang, W., Enhanced open circuit voltage of small molecule acceptors containing angular-shaped indacenodithiophene units for P3HT-based organic solar cells. Journal of Materials Chemistry C 2018, 6, 12347-12354.

(62) Tang, A.; Xiao, B.; Wang, Y.; Gao, F.; Tajima, K.; Bin, H.; Zhang, Z.-G.; Li, Y.; Wei, Z.; Zhou, E., Simultaneously Achieved High Open-Circuit Voltage and Efficient Charge Generation by Fine-Tuning Charge-Transfer Driving Force in Nonfullerene Polymer Solar Cells. Advanced Functional Materials 2018, 28, 1704507.

(63) Zhang, Q.; Xiao, B.; Du, M.; Li, G.; Tang, A.; Zhou, E., A2–A1–D–A1–A2 type non-fullerene acceptors based on methoxy substituted benzotriazole with three different end-capped groups for P3HT-based organic solar cells. Journal of Materials Chemistry C 2018, 6, 10902-10909.

(64) Yan, J.; Yi, Y.-Q.-Q.; Zhang, J.; Feng, H.; Ma, Y.; Wan, X.; Li, C.; Wei, Z.; Chen, Y., A privileged ternary blend enabling non-fullerene organic photovoltaics with over 14% efficiency. Journal of Materials Chemistry C 2020, 8, 15135-15141.

(65) Liu, S.; Zhao, B.; Cong, Z.; Cheng, Q.; Wang, W.; Pan, H.; Liu, J.; Wu, H.; Gao, C., Influences of the terminal groups on the performances of asymmetric small molecule acceptors-based polymer solar cells. Dyes and Pigments 2020, 178, 108388.

(66) Gao, W.; Wu, F.; Liu, T.; Zhang, G.; Chen, Z.; Zhong, C.; Zhu, L.; Liu, F.; Yan, H.; Yang, C., Multifunctional asymmetrical molecules for high-performance perovskite and organic solar cells. Journal of Materials Chemistry A 2019, 7, 2412-2420.

(67) Huang, C.; Liao, X.; Gao, K.; Zuo, L.; Lin, F.; Shi, X.; Li, C.-Z.; Liu, H.; Li, X.; Liu, F.; Chen, Y.; Chen, H.; Jen, A. K. Y., Highly Efficient Organic Solar Cells Based on S,N-Heteroacene Non-Fullerene Acceptors. Chemistry of Materials 2018, 30, 5429-5434.

(68) Chen, Y.; Liu, T.; Hu, H.; Ma, T.; Lai, J. Y. L.; Zhang, J.; Ade, H.; Yan, H., Modulation of End Groups for Low-Bandgap Nonfullerene Acceptors Enabling High-Performance Organic Solar Cells. Advanced Energy Materials 2018, 8, 1801203.

(69) Li, C.; Song, J.; Ye, L.; Koh, C.; Weng, K.; Fu, H.; Cai, Y.; Xie, Y.; Wei, D.; Woo, H. Y.; Sun, Y., High-Performance Eight-Membered Indacenodithiophene-Based Asymmetric A-D-A Type Non-Fullerene Acceptors. Solar RRL 2019, 3, 1800246.

(70) Zhu, J.; Xiao, Y.; Zhang, C.; Jia, B.; Lu, H.; Wang, J.; Lu, X.; Li, Z.; Zhan, X., Effects of alkoxylation position on fused-ring electron acceptors. Journal of Materials Chemistry C 2020, 8, 15128-15134.

(71) Li, T.; Wu, Y.; Zhou, J.; Li, M.; Wu, J.; Hu, Q.; Jia, B.; Pan, X.; Zhang, M.; Tang, Z.; Xie, Z.; Russell, T. P.; Zhan, X., Butterfly Effects Arising from Starting Materials in Fused-Ring Electron Acceptors. Journal of the American Chemical Society 2020, 142, 20124-20133.

(72) Liu, W.; Zhang, J.; Zhou, Z.; Zhang, D.; Zhang, Y.; Xu, S.; Zhu, X., Design of a New Fused-Ring Electron Acceptor with Excellent Compatibility to Wide-Bandgap Polymer Donors for High-Performance Organic Photovoltaics. Advanced Materials 2018, 30, 1800403.

(73) Zhang, J.; Liu, W.; Chen, S.; Xu, S.; Yang, C.; Zhu, X., One-pot synthesis of electron-acceptor composite enables efficient fullerene-free ternary organic solar cells. Journal of Materials Chemistry A 2018, 6, 22519-22525.

(74) Ming, R.; Zhang, M.; Gao, W.; Ning, W.; Luo, Z.; Zhong, C.; Zhang, F.; Yang, C., Fluorene-

fused ladder-type non-fullerene small molecule acceptors for high-performance polymer solar cells. Materials Chemistry Frontiers 2019, 3, 709-715.

(75) Duan, Y.-A.; Li, H.-B.; Geng, Y.; Wu, Y.; Wang, G.-Y.; and Su, Z.-M., Organic Electronics, 2014, 15, 602-613.

(76) Li, M.-Y.; Pan, Y.-Q.; Sun, G.-Y.; Geng, Y., The Journal of Physical Chemistry Letters, 2021, 12, 8982-8990.

(77) Lu, T.; Chen, F., Journal of Computational Chemistry, 2012, 33, 580-592.

(78) Liu, Y.; Li, M.; Yang, J.; Xue, W.; Feng, S.; Song, J.; Tang, Z.; Ma, W.; Bo, Z., Advanced Energy Materials, 2019, 9, 1901280.

(79) Frisch, M. J.; Trucks, G. W.; Schlegel, H. B.; Scuseria, G. E.; Robb, M. A.; Cheeseman, J. R.; Scalmani, G.; Barone, V.; Mennucci, B.; Petersson, G. A.; Nakatsuji, H.; Caricato, M.; Li, X.; Hratchian, H. P.; Izmaylov, A. F.; Bloino, J.; Zheng, G.; Sonnenberg, J. L.; Hada, M.; Ehara, M.; Toyota, K.; Fukuda, R.; Hasegawa, J.; Ishida, M.; Nakajima, T.; Honda, Y.; Kitao, O.; Nakai, H.; Vreven, T.; Throssel, K.; Montgomery, J. A., Jr.; Peralta, J. E.; Ogliaro, F.; Bearpark, M.; Heyd, J. J.; Brothers, E.; Kudin, K. N.; Staroverov, V. N.; Kobayashi, R.; Normand, J.; Raghavachari, K.; Rendell, A.; Burant, J. C.; Iyengar, S. S.; Tomasi, J.; Cossi, M.; Rega, N.; Millam, J. M.; Klene, M.; Knox, J. E.; Cross, J. B.; Bakken, V.; Adamo, C.; Jaramillo, J.; Gomperts, R.; Stratmann, R. E.; Yazyev, O.; Austin, A. J.; Cammi, R.; Pomelli, C.; Ochterski, J. W.; Martin, R. L.; Morokuma, K.; Zakrzewski, V. G.; Voth, G. A.; Salvador, P.; Dannenberg, J. J.; Dapprich, S.; Daniels, A. D.; Farkas, Ö.; Foresman, J. B.; Ortiz, J. V.; Cioslowski, J.; Fox, D. J. *Gaussian 09 Rev. D.01*; Gaussian, Inc.: Wallingford, CT, 2009.